Synthesis, Structures and Properties of Luminescent (C^N^C)gold(III) Alkyl Complexes: Correlation between Photoemission Energies and C-H Acidity

Julio Fernandez-Cestau,* Benoit Bertrand, Anna Pintus and Manfred Bochmann*
School of Chemistry, University of East Anglia, Norwich, NR4 7TJ. UK.
Fax: +44 016035 92044; E-mail: m.bochmann@uea.ac.uk

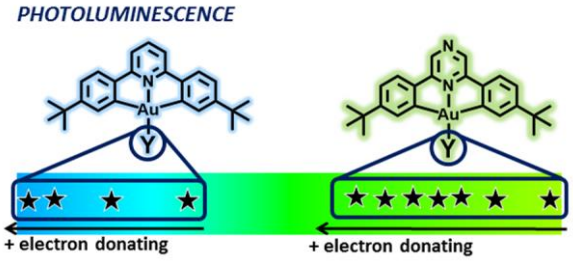

ABSTRACT: The reaction of (C^N^{pz}^C)AuCl with C-H acidic compounds $H_2CR^1R^2$ in the presence of base readily affords the corresponding alkyl complexes (C^N^{pz}^C)AuCHR^1R^2 [**2a**, $R^1 = R^2$ = CN; **3a**, $R^1 = R^2$ = C(O)Me; **4**, $R^1 = R^2$ = CO_2Et; **5**, $R^1 = R^2$ = C(O)Ph; **6a**, R^1 = H, R^2 = C(O)Me]. The analogous pyridine-pincer complexes **2b**, **3b** and **6b** were obtained similarly [C^N^{pz}^C = 2,6-bis(4′-^{t}BuC_6H_3)$_2$pyrazine dianion; C^N^{py}^C = 2,6-bis(4′-^{t}BuC_6H_3)$_2$pyridine dianion]. The reactions of (C^N^{pz}^C)AuOAc^F (**7a**) and (C^N^{py}^C)AuOAc^F (**7b**) with MeMgI gave the methyl complexes (C^N^{pz}^C)AuMe (**8a**) and (C^N^{py}^C)AuMe (**8b**), respectively. The crystal structures of **2a**, **2b**, **3a**, **6a**, and **7a** have been determined. The photophysical properties of the new complexes and those of the previously reported gold hydride (C^N^{pz}^C)AuH (**AuH**) are reported. The lower-energy absorption and the emission maxima follow the energy sequence **2a** < **3a** < **4** < **5** < **6a** < **AuH** ≈ **8a** for the pyrazine series, and **2b** < **3b** < **6b** ≈ **8b** for the pyridine series. These values provide a correlation with the pK_a values of the corresponding ancillary ligand precursors. In agreement with DFT calculations, the emissions are assigned to ^{3}IL(C^N^C)/^{3}ILCT {(C_6H_4^{t}Bu-4')→pz/py*} transitions, dominated by the HOMO and the LUMO orbitals. The LUMO is located in the heterocycle (py/pz) in *trans* position to the ancillary ligand, which makes this orbital more sensitive to the electronic nature of the ancillary ligand than the HOMO. The calculations establish that the charge transfer from the *t*BuC_6H_3 ligand fragments to the central heterocycle ring in the dominant transition explains the modulation of the properties with the σ-donor characteristics of the alkyl or hydride ligands.

Keywords: Gold complexes, Pincer complexes, Metal alkyls, Photoluminescence, Crystal structure

Introduction

Cyclometalated Gold(III) complexes, particularly those based on cyclometalated bidentate 2-arylpyridine (C^N) and tridentate 2,6-diarylpyridine ligands (C^N^C) have proved to be highly successful ligand platforms in Au(III) chemistry, since they impart good thermal stability and protect the gold(III) centers against reduction.[1] Complexes of this type also exhibit rich photophysical properties that form the basis for application as sensors, bioimaging agents and as emitter materials in organic light-emitting diodes (OLEDs).[2]

However, in (C^N^C)AuY complexes the presence of ^{3}LMCT (ligand-to-metal charge transfer) and ^{3}dd excited states can provide effective deactivating pathways for the photoemissions in these systems.[3,4] This has limited the range of photoluminescent complexes almost exclusively to those with strong carbon-based σ-donors in the ancillary positions, such as Y = alkyl, aryl, alkynyl, cyanide or *N*-heterocyclic carbenes.[5-7] These strong σ-donating ligands push the gold 5d σ* orbital to higher energies, so that the emissive ^{3}IL(C^N^C) transitions centered on the pincer π-system become accessible. The colour of the emission is determined by the electronic properties of the cyclometallated ligand. The successful modulation of the photoluminescence (PL) wavelengths by ligand design and varying the combination of substituens has also been reported.[8,9] However, with this approach the synthesis protocol of each complex has to be optimized individually, including the time consuming optimization of the mercuration and transmetallation steps.

In some of these cases, and depending on the ancilliary ligand Y, a contribution of ligand-to-ligand charge transfer (LLCT) to the emission has been also observed. This is particulary true for the extensively studied family of cyclometalated (C^N^{py}^C) gold alkynyl complexes.[10,11] A wide range of alkynyl substituents has been used to modulate emission energies.[12] However, the success of this strategy has been limited for two main reasons: (a) if the emission of the system is purely centered on the cyclometallated ligand, the presence of different substituents on the alkynyl ligand has little effect on the relative energy of the C^N^C centered orbitals; and (b) if there is a relevant LLCT (C^N^C → C≡CR) contribution, it becomes difficult to predict the colour of the emission on the basis of the electronic properties of the substituents of the alkynyl ligands, as many other factors affect the transition energy.

We recently demonstrated that the pyrazine-based (C^N^{pz}^C)Au^{III}Y pincer complexes show a wider reactivity than the pyridine analogues, since Y may readily be varied under mild conditions. Also, Y = aryl, alkynyl or NHC donors are not necessarily required in order to generate photoemissive materials; e.g. for the pyrazine series even the chloride is photoemissive at room temperature.[13,14] Beyond photoluminescence, (C^N^{pz}^C)Au^{III} compounds are of interest as anti-tumor agents.[15] A remarkable case for the difference in PL of pyridine- vs. pyrazine-based (C^N^C) gold complexes are the thiolates, (C^N^C)AuSR, which are strongly photoemissive whereas their pyridine analogues are non-emissive at room temperature. The photoluminescence of (C^N^{pz}^C)AuSR was due to

^{3}IL(C^N^{pz}^C) emissions which, unusually, proved to be modulated by pyrazine-pyrazine aggregation leading to bimolecular emissive states.[16]

As an extention to these studies, we became interested in the luminescence behavior of gold(III) alkyl complexes and report here the synthesis and PL properties of a family of compounds (C^N^{pz}^C)AuY [**2a**, Y = $CH(CN)_2$; **3a**, Y = $CH\{C(O)Me\}_2$; **4**, Y = $CH(CO_2Et)_2$; **5**, Y = $CH\{C(O)Ph\}_2$; **6a**, Y = $CH_2C(O)Me$; **8a**, Y = Me; **AuH**, Y = H] and the analogous pyridine-pincer complexes **2b**, **3b, 6b** and **8b** (C^N^{pz}^C = [2,6-bis(4'-*t*-$BuC_6H_3)_2$pyrazine]$^{2-}$; C^N^{py}^C = [2,6-bis(4'-*t*-$BuC_6H_3)_2$pyridine]$^{2-}$). The synthesis can be carried out under mild conditions and offers a good alternative to the alkynyl and NHC ancilliary ligands used to activate photoluminescence in cyclometallated Au(III) systems. The emission energy can be modulated and predicted by the double strategy of altering the heterocyclic core of the cyclometallated ligand, as well as by fine-tuning the electronic properties of the Y ligand.[17]

Results and Discussion

Synthesis and Characterization. Gold(III) alkyl complexes bearing pyrazine- and pyridine-based C^N^C pincer ligands were prepared from C-H acidic hydrocarbons in the presence of base. In all cases C-coordinated complexes were obtained. The activation of (C^N^C)AuCl with potassium *tert*.-butoxide in toluene and subsequent reaction with an excess of hydrocarbons $H_2CR^1R^2$ proved quite facile and general and follows a procedure reported previously for the synthesis of (C^N^{pz}^C)Au-pyrazole (Scheme 1).[18] While potassium carbonate proved to be a strong enough base to generate **6a**, formation of the pyridine complex **6b** required a stronger base, KO^{t}Bu, which demonstrates the higher reactivity of the pyrazine complex **1a** compared to its pyridine analogue **1b**, a feature previously observed in ligand substitutions with thiols.[16] On the other hand, less acidic hydrocarbons like ethyl acetate and acetonitrile proved unreactive even in the presence of KO^{t}Bu for both systems.

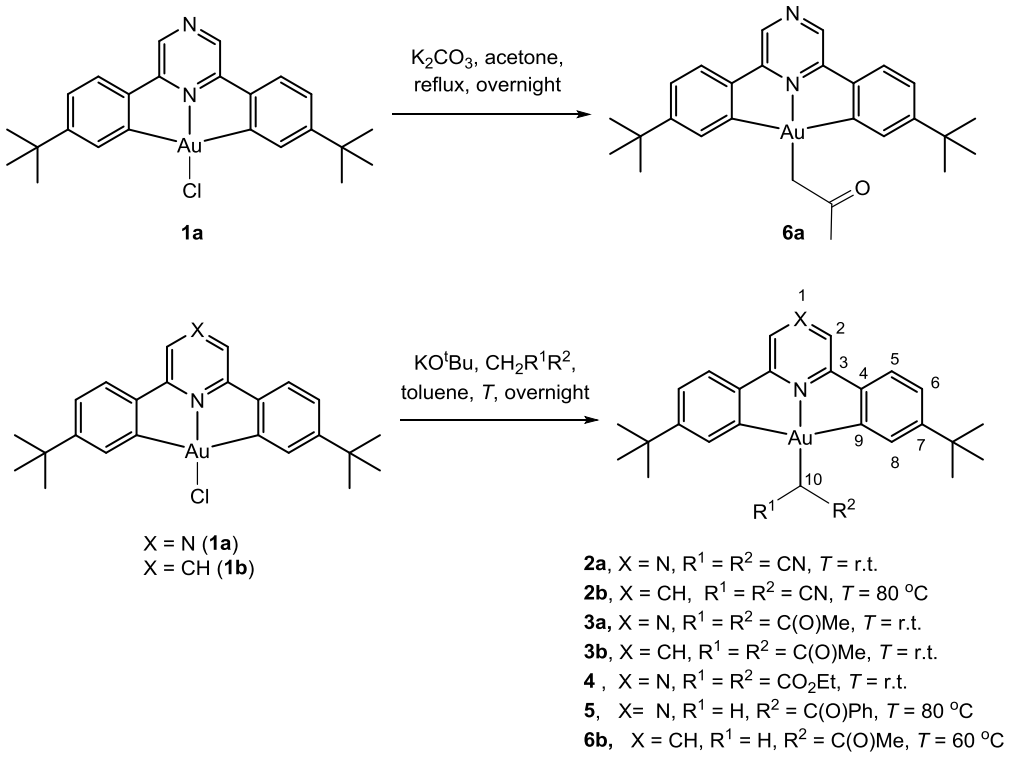

Scheme 1: Synthesis of complexes **2 - 6**, showing the numbering scheme used for NMR assignments.

The formation of these compounds was confirmed by ^{1}H, $^{13}C\{^{1}H\}$ NMR and IR spectroscopy techniques. All ^{1}H NMR spectra showed signals for H^{8} in the region of δ 7.9. Complexes **2 - 4** show singlets integrating for one proton for the alkyl-CH moiety (H^{10}) at δ 3.64 (**2b**), 3.68 (**2a**), 4.69 (**3b**) and 4.96 ppm (**3a** and **4**). While both methyl groups appeared equivalent in the ^{1}H NMR spectra of both **3a** and **3b**, as indicated by a single resonance integrating for six protons at δ 2.29 and 2.31, respectively, in the ^{1}H NMR spectrum of **4** the ethyl-CH_2 groups are inequivalent, giving rise to a multiplet at δ 4.09, instead of a quadruplet, as was previously found in case of Pt(II) complexes.[19] In the infrared spectra of **2 - 4**, the respective C≡N and C=O stretching frequencies are observed at 2237 cm^{-1} (**2a**), 2233 cm^{-1} (**2b**), 1677 cm^{-1} (for **3a** and **3b**), and 1737 and 1732 cm^{-1} (**4**). The presence of two C=O bands in the IR spectrum of **4** confirms the inequivalence of the ester moieties observed in the ^{1}H NMR spectrum.

Complexes **5**, **6a** and **6b**, show singlets integrating for two protons corresponding to H^{10}, at δ 3.65 (**5**) and 3.11 (**6a** and **6b**). The compounds show intense C=O vibrations at 1654 cm^{-1} and 1674 cm^{-1} for **5** and **6a/b**, respectively.

Crystals suitable for X-ray diffraction were grown for complexes **2a**, **2b**, **3a, 6a** and **7a**. There are three different molecules of **3a** in the asymmetric unit. One of them is depicted in Figure 1b, and selected distances and angles are given in the legend. The other two molecules show similar structural parameters. The metal center has a square-planar environment, as expected for Au(III), distorted to

accommodate the strained cyclometallated ligand. The fourth coordination site is occupied by the acetylacetonate. Unlike $R_2Au(acac)$ complexes (R = Me, aryl), where the pentanedionato ligands are O-bonded,[20] the structure of **3a** confirms the coordination through the σ-C bond of the central carbon. The Au-C25 distance (2.078(5) Å) is in the range of values observed for other complexes with Au(III)-C(sp^3) bonds.[21,22] The main difference between the three independent molecules in the asymmetric unit cell is the N1-Au-C25-H25 torsion angle, which is 25° for molecule 1 (Figure 1b), and 24° and 58° for the other two molecules.

The disposition of the acetylacetonyl ligands in these molecules is determined by the requirement to accommodate intermolecular interactions in the solid state. These interactions are mainly O···H hydrogen bonds that involve the oxygen atoms of the acetylacetonate ligands and H atoms of neighboring molecules. In addition, the crystal lattice shows the presence of large voids, which are occupied by hexane molecules, with positional disorders so that they could not be included in the model. The analysis with PLATON reveals a volume of 591 $Å^3$ for this void. Using SQUEEZE to address these disorder problems resulted in two hexane molecules in the unit cell.

The crystal structure of **6a** is depicted in Figure S2, and selected distances and angles are given in the legend. The structural parameters are very similar to those of complex **3a**, including the Au-C25 distance of 2.058(3) Å, typical for Au-C alkyls.

In the crystal structure of **2a** the first feature to note is the existence of a positional disorder in the carbon atom of the $CH(CN)_2$ ligand. This atom is equally positioned in two very similar locations that have been defined as C25A and C25B. The structural parameters are very similar between both; in Figure 1a we show the one corresponding to C25A. For both malonitrile complexes **2a** (Figure 1a) and **2b** (Figure S1) the reduced donor character of the -$CH(CN)_2$ ligand is reflected in the relatively long Au-C(alkyl) distances of 2.11(2) Å (**2a**) and 2.084(4) Å (**2b**), compared to an Au-Et distance of 2.042(8) Å in (C^N^{py}^C)AuEt.[22]

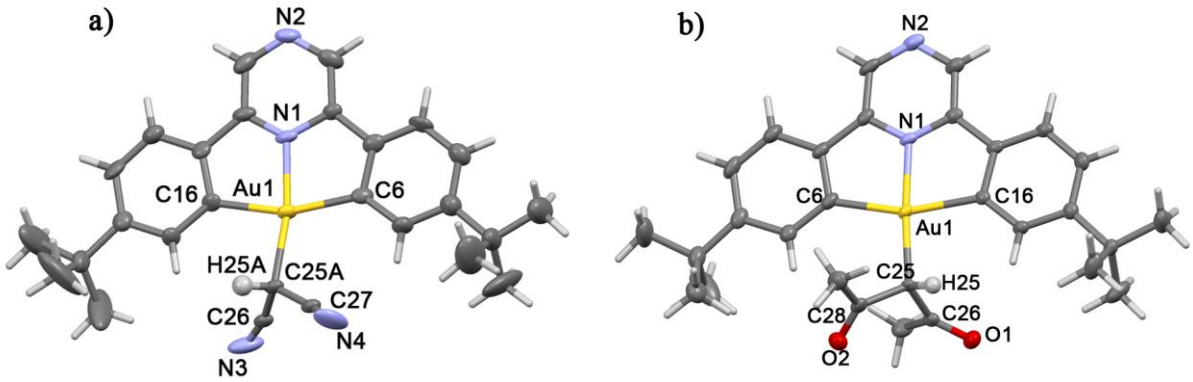

Figure 1. (a) Structure of **2a**. Selected bond distances (Å) and angles (°): Au-C25A 2.11(2), Au-C6 2.073(9), Au-C16 2.09(1), Au-N1 2.009(8), N1-Au-C25A 166.8(6), N1-Au-C6 81.0(3), N1-Au-C16

79.8(3), C6-Au-C25A 106.4(6), C16-Au-C25A 92.5(2); torsion angle N1-Au-C25A-H25A 9°. (b) Structure of **3a**: Au-C25 2.078(5), Au-C6 2.095(4), Au-C16 2.083(4), Au-N1 2.021(4), N1-Au-C25 175.2(2), N1-Au-C6 80.3(2), N1-Au-C16 80.5(2), C6-Au-C25 104.4(2), C16-Au-C25 94.8(2); torsion angle N1-Au-C25-H25 25°.

To extend the series of alkyl subsituents to more strongly electron-donating alkyls we synthesized the methyl derivatives **8a** and **8b** by reacting the corresponding trifluoroacetate complexes **7a** and **7b** with MeMgBr in THF, by adaptation of previously reported protocols (Scheme 2).[22,23] The X-ray structure of **7a** (see SI, Figure S3) is very similar to the one previously reported for the pyridine analogue.

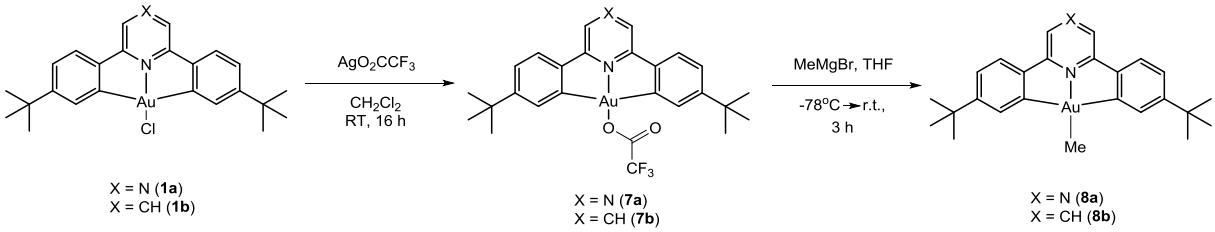

Scheme 2: Synthesis of complex **8a** - **b**.

Compared to the chloride **1a**, complex **7a** is characterized by a shift in the ^{1}H NMR signal of the H^8 proton by $\Delta\delta$ -0.48 ppm. The IR spectrum shows the typical C=O band of trifluoroacetate at 1727 cm^{-1}. The formation of complex **8a** was confirmed by ^{1}H NMR spectroscopy, the data resemble those of the previously reported complex **8b**.[22]

Photophysical Properties. The photophysical properties of the complexes are conditioned by the cyclometalated ligand. The most relevant feature in the UV-Vis absorption spectra is the low-energy band characteristic of this type of complexes and typically attributed to ^{1}IL(C^N^C) transitions (Table 1).

The pyrazine complexes are significantly more strongly emissive than their pyridine analogues. In polymeric media the complexes show emission profiles that resemble those observed in the solid state, but with narrower bands, higher intensities and better resolution. The photophysical properties of the complexes in the solid state, in poly(methylmethacrylate) (PMMA) containing 10 wt-% Au compound, and in dichoromethane solution are collected in Table 2. The emissions of **2b** and **3b** in a PMMA matrix were too weak to be measured. Both the low-energy absorptions and the emissions of the pyrazine complexes are red-shifted compared to the pyridine analogues, as expected. This shift reflects the differences in the π-π^* energy gap, which is 0.95 eV lower for pyrazine than for pyridine.[24] The emissions are assigned to ^{3}IL(C^N^C) transitions. This is in line with the C^N^C vibronic progression of the spectra in all cases, which is similar in energy to the vibronic progression of the low energy absorptions.

When comparing complexes of the same cyclometalated C^N^C ligand, the wavelengths of the low energy absorption band follow the trend: **2a** < **3a** < **4** < **5** < **6a** < **8a** in the pyrazine series. This parallels the pyridine series: **2b** < **3b** < **6b** < **8b** (see Figure 2a). The emission maxima are similarly affected by the electronic nature of the ancillary ligand Y. In the solid state the shift is not clearly noticeable, presumably due to the fact that the bands do not show a good spectral definition. However, in CH_2Cl_2 glass at 77 K the emissions show the same trend as the absorptions: **2a** (548 nm) < **3a** (540 nm) < **4** (532nm) < **5** (528 nm) < **6a** (524 nm) < **8a** (520 nm) (Figure 2b).

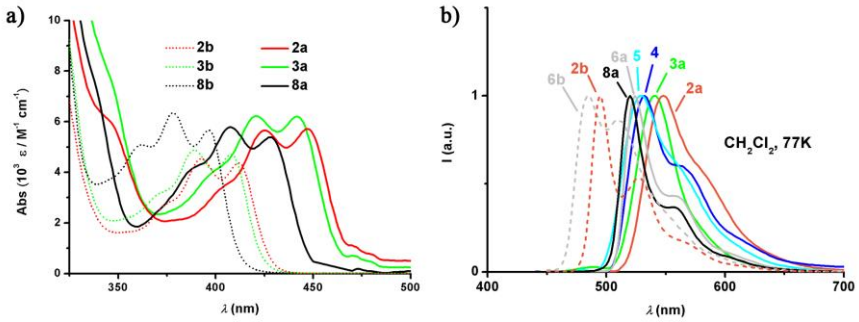

Figure 2. (a) Low energy UV-Vis absorption spectra of complexes **2a**, **2b**, **3a**, **3b**, **8a** and **8b** in CH_2Cl_2 (10^{-5} *M*) at 298 K. (b) Emission spectra of **2a**, **2b**, **3a**, **4**, **5**, **6a**, **6b** in CH_2Cl_2 (10^{-4} *M*) at 77 K.

The recently reported[25] gold(III) hydride complex (C^N^{pz}^C)AuH (**AuH**) also fits into this series. **AuH** in PMMA (10 wt-%) shows an intense green emission due to a ^{3}IL(C^N^{pz}^C) transition, with a high quantum yield (10.3 %) (Figure 3). This is, to the best of our knowledge, the first case of a gold hydride complex (in any oxidation state) showing photoluminescent properties.

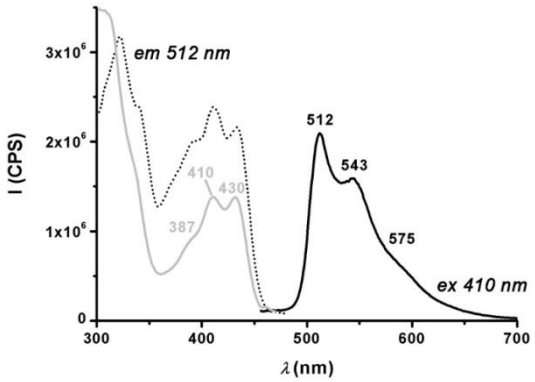

Figure 3. Emission (black solid line) and excitation (black dotted line) bands of (C^N^{pz}^C)AuH (**AuH**) in PMMA (10 wt.-%), and UV-Vis absorption spectrum (grey line) of **AuH** in CH_2Cl_2 (10^{-5} *M*) at 298 K.

These absorption and emission data show that there is a correlation of the low-energy absorption bands and of the emission energies (in CH_2Cl_2 at 77K and in PMMA at room temperature) with the pK_a values of the alkyl ligand precursors in DMSO and of H_2 [pK_a = 11.1 (malodinitrile; **2a/b**), 13.3 (acetylacetone; **3a/b**), 16.4 (diethylmalonate; **4**), 24.7 (acetophenone; **5**), 26.5 (acetone; **6a/b**), 36 (H_2; **AuH**)] (Figure 4). As will be discussed in the computational section, this is a reflection of the fact that the LUMO is more destabilized in energy compared to the HOMO, in response to the electron-donating properties of the ancillary ligands. Increasing the pK_a further, to 56 (CH_4) as in compounds **8a/b**, results in only small further shifts in the absorption and emission maxima.

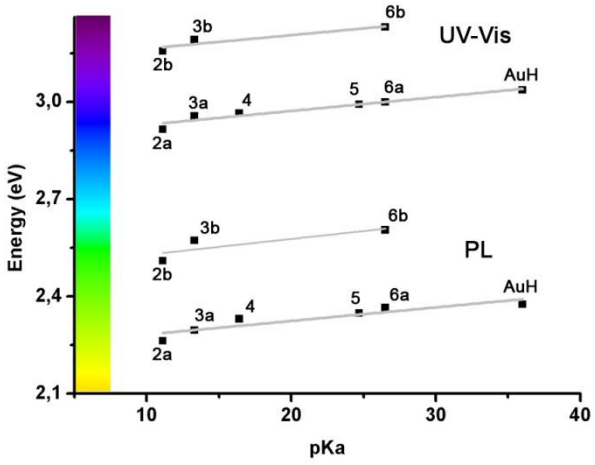

Figure 4. Correlation of the pK_a values of hydrocarbons in DMSO with the lowest energy absorption for each complex (eV; calculated by averaging the three low energy absorption bands for each complex) and with the emission maxima in CH_2Cl_2 solution at 77 K. Grey lines represent the linear regression for each series of data with slopes of about 0.004 eV/pK_a.

In CH_2Cl_2 solution at room temperature the situation is more complex. As can be seen in Figure 5 for some illustrative examples, the emission is the result of the sum of two components: the ^{3}IL(C^N^C) emission together with a high-energy feature. This high-energy feature, marked with an asterisk in Figure 5, appears in a different proportion with respect to the main band, depending on the complex. For the pyrazine complexes in some cases it is very weak (**8a**) or appears as a small shoulder (**5**), but is prominent in some complexes (**2a**). For the pyridine series the ^{3}IL(C^N^C) emission is only present in some cases (**8b**) and in others the weak emission that is observed has only the high energy component (**2b**). This high energy band can be tentatively ascribed to ^{1}IL(C^N^C) transitions. This is confirmed by the fact that bubbling air through the solution increases, in all cases, the proportion of this band with respect to the phosphorescence, and becomes the only emissive pathway for all the complexes under aerobic conditions.

The energy of the ^{3}IL(C^N^C) band in fluid media also follows the trend of the electronic properties of the ancilliary ligands found in PMMA and in frozen CH_2Cl_2 at 77 K (for example 528 nm **2a** < 520 nm **5** < 511 nm **8a**). As mentioned before, the pyridine series shows higher energy emissions compared to the pyrazine analogues. This is true not only for the triplet emissions (for example 511 nm **8a** vs. 471 nm **8b**) but also for the higher energy ^{1}IL(C^N^C) transitions (484 nm **2a** vs. 440 nm **2b**) and further supports this assignment.

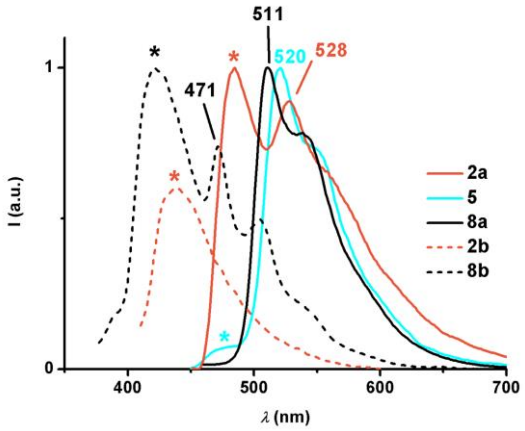

Figure 5. Emission spectra of complexes **2a**, **5**, **8a**, **2b**, **8b** in CH_2Cl_2 (10^{-4} *M*) at 298 K.

Table 1: Absorption data for complexes **2 - 8** in CH_2Cl_2 (10^{-5} *M*)

Complex	Absorbance [nm] (10^3 ε/M^{-1} cm^{-1}). // Low energy absorption average [eV]
(C^N^{pz}^C)Au{$CH(CN)_2$} **2a**	281 (19.5), 319 (10.7), 345 (5.9), 406 (3.8), 425 (5.3), 447 (5.6) // 2.91_5
(C^N^{pz}^C)Au{$CH(C(O)Me)_2$} **3a**	293 (19.5), 319 (15.5), 340*sh* (9.0), 399 (4.0), 419 (6.2), 442 (6.2) // 2.95_7
(C^N^{pz}^C)Au{$CH(CO_2Et)_2$} **4**	286 (19.5), 317 (13.1), 340*sh* (7.8), 397 (4.1), 418 (6.0), 442 (5.8) // 2.96_5
(C^N^{pz}^C)Au{$CH_2(COPh)$} **5**	286 (18.2), 320 (12.8), 339*sh* (8.0), 395 (4.2), 415 (5.6), 435 (5.4) // 2.99_2
(C^N^{pz}^C)Au{$CH_2C(O)Me$} **6a**	263 (24.3), 288 (14.0), 321 (9.7), 341 (6.3), 392 (3.7), 415 (4.5), 435 (4.4) //3.00_0
(C^N^{pz}^C)AuCH_3 **8a**	280 (20.0), 287 (16.2), 337*sh* (7.8), 389 (4.2), 407 (5.8), 428 (5.4) // 3.04_4
(C^N^{pz}^C)AuH **AuH**	282 (18.6), 285 (18.0), 338*sh* (8.1), 387 (4.0), 410 (5.5), 430 (5.3) // 3.03_7
(C^N^{py}^C)Au{$CH(CN)_2$} **2b**	280 (21.5), 309*sh* (11.7), 376 (2.8), 392 (4.5), 412 (4.4) // 3.15_7
(C^N^{py}^C)Au{$CH(C(O)Me)_2$} **3b**	281 (18.7), 308*sh* (12.8), 370 (3.1), 389 (4.9), 408 (4.7) // 3.19_2
(C^N^{py}^C)Au{$CH_2C(O)Me$} **6b**	294 (15.3) , 318*sh* (12.0), 366 (3.7), 385 (5.3), 402 (4.9) // 3.23_1
(C^N^{py}^C)AuCH_3 **8b**	295 (17.2) , 315*sh* (13.0), 362 (5.1), 378 (6.4), 396 (5.6) // 3.27_9

Table 2. Emission properties in the solid state, PMMA (10 %) and in CH_2Cl_2 solution (10^{-3} *M*) at 298 K and 77 K.

Complex		λ_{em} / nm (λ_{ex} / nm) {ϕ / % (λ_{ex})}	
		298 K	77 K
2a	Solid	520_{max}, 541, 586*sh* (300-450)	519_{max}, 553, 585*sh* (380)
	CH_2Cl_2	484_{max}, 528, 553*sh*, 600*sh* (377, 477)	546_{max}, 576*sh* (380)
	PMMA	528_{max}, 557*sh* (320-430) {6.2 (415)}	
3a	Solid	476*sh*, 520_{max}, 546*sh* (350-460)	518_{max}, 550*sh*, 582*sh* (370)
	CH_2Cl_2	480, 522, 550*sh* (369, 467)	492*sh*, 540_{max}, 562*sh* (380)
	PMMA	523-554 (320-430) {< 1 (415)}	
4	Solid	475*sh*, 520_{max}, 545*sh* (300-450)	517_{max}, 552, 588*sh* (370)
	CH_2Cl_2	484, 532_{max}, 554*sh* (370, 464)	532_{max}, 558*sh*, 602*sh* (370)
	PMMA	524_{max}, 552*sh* (320-430) {6.1 (415)}	
5	Solid	520_{max}, 546*sh* (325, 345, 397, 416, 440)	518, 560 (370)
	CH_2Cl_2	475*sh*, 520_{max}, 542*sh* (365, 459_{max})	484*sh*, 528_{max}, 556*sh* (380)
	PMMA	524, 560_{max} (320-430) {< 1 (415)}	
6a	Solid	475*sh*, 520_{max}, 546*sh* (378, 403, 430-455)	518_{max}, 549*sh*, 580*sh* (370)
	CH_2Cl_2	503*sh*, 518_{max}, 551, 590*sh* (380-420)	524_{max}, 552*sh* (370)
	PMMA	519_{max}, 547*sh* (320-430) {8.6 (415)}	
8a	Solid	520_{max}, 542*sh* (300-420)	518_{max}, 550*sh*, 580*sh* (370)
	CH_2Cl_2	511_{max}, 536*sh*, 582*sh* (300-420)	520_{max}, 550*sh* (370)
	PMMA	508_{max}, 536*sh*, 574*sh* (320-430) {3.2 (415)}	
AuH	Solid	517_{max}, 542, 577*sh* (320-430)	520_{max}, 550*sh*, 577*sh* (370))
	CH_2Cl_2		522_{max}, 552*sh*, 5780*sh* (370))
	PMMA	512_{max}, 543, 575*sh* (320-430) {10.3 (415)}	
2b	Solid	No emissive	536_{max}, 562*sh* (320-430)
	CH_2Cl_2	440*br* (370)[a]	494_{max}, 529, 555*sh* (370)
	PMMA	[a]	
3b	Solid	449_{max}, 473*sh* (370)[a]	478_{max}, 514, 542*sh* (370)
	CH_2Cl_2	451*br* (370)[a]	448*sh*, 477_{max}, 506*sh* (380)
	PMMA	[a]	
6b	Solid	474_{max}, 510, 542, 572*sh* (370)	474_{max}, 510, 542*sh*, 562*sh* (370)
	CH_2Cl_2	442, 473, 498*sh*, 533*sh* (350-420)	477_{max}, 505*sh*, 542*sh* (380)
	PMMA	444*sh*, 475_{max}, 506, 533*sh* (310-410) {< 1 (400)}	
8b	Solid	472_{max}, 507 (310-400)	472_{max}, 507, 540*sh* (370)
	CH_2Cl_2	423_{max}, 471, 505, 535*sh* (300-400)	474_{max}, 500, 530*sh* (370)
	PMMA	474_{max}, 507, 532*sh*, 578*sh* (310-400) {< 1 (400)}	

[a] Weak emission.

Theoretical Calculations. Computations have been performed at the density functional theory (DFT) level with the aim of rationalizing the correlation of the low energy absorption and the

emission maxima with the electronic properties of the ancilliary ligand. To reduce the complexity of the systems, the *t*Bu substituents of the cyclometallated ligands have been omitted. We refer to this with an asterisk next to each complex number. Details of the calculations can be found in the SI.

These calculations establish that the lower energy absorption, related to the $S_0 \rightarrow S_1$ transition, can be assigned in all cases to an almost pure HOMO-LUMO monoelectronic excitation (see Table S2). As can be seen in Figures S6 and S7, in all cases the HOMO is localized in the pincer with only a small contribution from the Au center. The LUMO, in contrast, is mainly centered on the heterocyclic central ring (see Figure 6 for an illustrative example for **2a***).

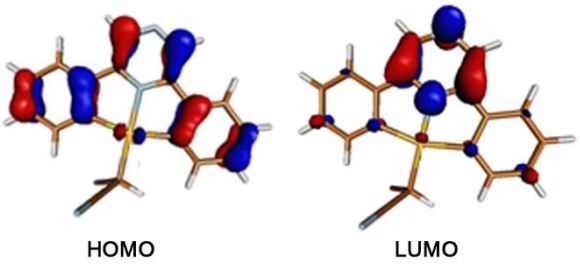

Figure 6. Frontier molecular orbitals of complex **2a***.

Both frontier molecular orbitals are raised in energy as the electron-donating character of the σ-bonded ligand Y increases (Table 3). However, since the LUMO is centered on the central heterocycle (pyridine or pyrazine) the ligand *trans* to this ring has a strong influence on its energy. The LUMO is therefore destabilized to a larger extent than the HOMO, resulting in an increased HOMO-LUMO gap with increasing electron-donating character of Y (for example 4.14 eV **2a*** *vs*. 4.20 eV **6a***).

Table 3. Calculated energy values of frontier Kohn-Sham molecular orbitals (KS-MOs) and energy difference *ΔE* between KS-HOMO and KS-LUMO (eV) in dichloromethane solvent model (IEF-PCM SCRF model).

Complex	**2a***	**3a***	**4***	**5***	**6a***	**AuH***	**8a***	**2b***	**3b***	**6b***	**8b***
HOMO	-6.92	-6.80	-6.78	-6.75	-6.74	-6.72	-6.68	-6.76	-6.64	-6.58	-6.52
LUMO	-2.79	-2.65	-2.61	-2.55	-2.54	-2.49	-2.42	-2.38	-2.25	-2.14	-2.02
ΔE	4.14	4.15	4.17	4.20	4.20	4.23	4.26	4.38	4.39	4.44	4.50

As can be seen in Figures 7a and 7b, for both the pyrazine and the pyridine series there is a linear correlation between the experimental lowest energy absorption band of the complexes in CH_2Cl_2 with the calculated HOMO-LUMO gaps. Given that, as mentioned above, the $S_0 \rightarrow S_1$ transitions were found to be almost pure HOMO-LUMO excitations, a similar correlation is found between the experimental

absorptions and these transitions (see Figures S8 and S9). While these calculations work provide a good model for such subtle chemical modifications, we did notice a general tendency to slightly overestimate (by about 8%) the energy of the $S_0 \rightarrow S_1$ transition compared with the experimental absorption bands; point checks showed that this overestimation is reduced to ~ 5% if the *t*Bu substituents are included in the model.

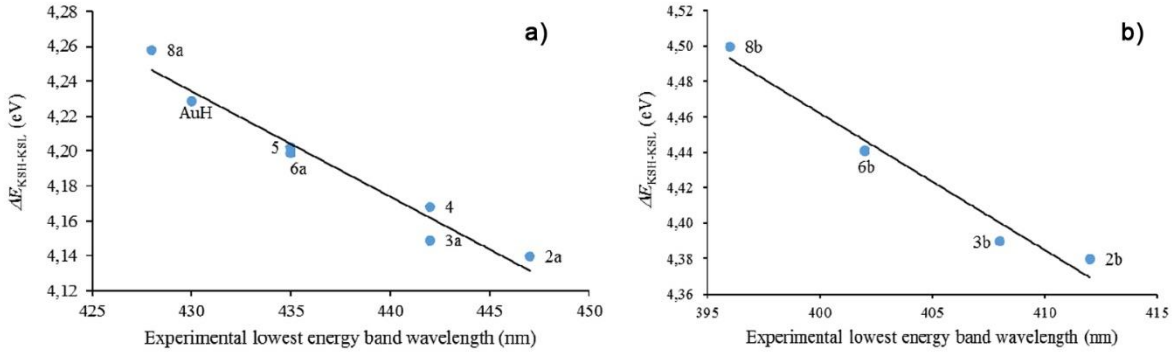

Figure 7. Correlation between the calculated HOMO-LUMO energy difference ΔE (eV) (IEF-PCM SCRF model) and the experimental lowest energy absorption bands in CH_2Cl_2 (nm) for (a) **2a***, **3a***, **4***, **5***, **6a***, **8a*** and **AuH*** (R^2 = 0.958). (b) **2b***, **3b***, **6b***, and **8b*** (R^2 = 0.966).

Conclusion

A new family of luminescent pyrazine-based alkylgold pincer complexes (C^N^{pz}^C)Au^{III}Y is readily accessible under mild, aerobic reactions conditions by reacting gold(III) halides with C-H acidic functionalized hydrocarbons HY in the presence of base. These reactions cover a pK_a scale from 11 to 26.5. The alkylation of (C^N^{pz}^C)AuOAc^F with methyl Gignard reagents to give the methyl complex extends the pK_a scale to 56. Pyridine-based pincer complexes are similarly accessible. The pyrazine complexes show green to yellow photoluminescence in the solid state and in solution, with in most cases significantly higher intensities than the pyridine analogues. Excitation involves intra-ligand charge transfer from the phenyls to the central heterocyclic ring of the C^N^C framework. In accord with DFT calculations the luminescence is assigned to ^{3}IL(C^N^C)/^{3}ILCT {(C_6H_4^{t}Bu-4)→pz/py*} transitions. This internal charge transfer has been postulated as crucial for understanding the photophysical properties of Au(III) complexes with pincer ligands;[4] here we show that this internal charge transfer process can be employed to systematically modulate the photophysics of this type of complexes.

The change of the heterocycle in the pincer ligand defines the energy band of the emissions but, for a given pincer, the emission color can be fine-tuned by changing the electronic properties of the alkyl ligand. These subtle changes in emission energies can be rationalized on the basis of a simple chemical parameter; the pK_a values of the hydrocarbons HY. The (C^N^{pz}^C) gold hydride was also

shown to be photoluminescent and fits within the pK_a series. The effect is related to the *trans* influence of the Y ligand and the fact that the LUMOs in these complexes are mainly located on the heterocycle *trans* to Y; the Y ligand raises the LUMO level and increases the HOMO-LUMO gap.

Experimental

When required, manipulations were performed using standard Schlenk techniques under dry nitrogen or using an M. Braun glove box. Nitrogen was purified by passing through columns of supported P_2O_5 with moisture indicator, and of activated 4 Å molecular sieves. Anhydrous solvents were freshly distilled from appropriate drying agents. Infrared spectra were recorded using a Perkin Elmer Spectrum 65 FT-IR spectrometer with a diamond ATR attachment. Elemental analyses were carried out at London Metropolitan University. ^{1}H, ^{13}C{^{1}H} and ^{19}F spectra were recorded using a Bruker Avance DPX-300 spectrometer. $CDCl_3$, CD_2Cl_2 and DMSO-d_6 were dried over CaH_2, degassed by three freeze-pump-thaw cycles and stored on 4 Å molecular sieves prior to use. ^{1}H NMR spectra (300.13 MHz) were referenced to the residual protons of the deuterated solvent used. ^{13}C{^{1}H} NMR spectra (75.47 MHz) were referenced internally to the D-coupled ^{13}C resonances of the NMR solvent. ^{19}F{^{1}H} NMR spectra (282.38 MHz) were referenced to $CFCl_3$. Complexes **7b** and **8b** were synthesized by modifiying reported procedures.[22] The assignment of the signals for the C^N^C ligand framework is as shown in Figure 8. Compounds **2** – **6** were synthesized without exclusion of air and moisture, compounds **7** and **8** were prepared under dry nitrogen.

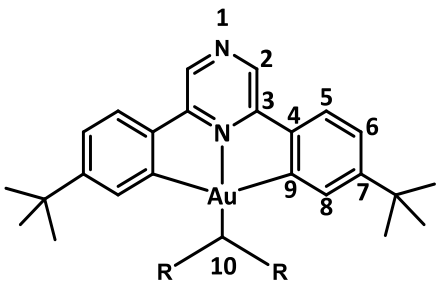

Figure 8. Numbering scheme of the C^N^C ligand.

(C^N^{pz}^C)Au{CH(CN)$_2$} (2a)

A mixture of (C^N^{pz}^C)AuCl (50 mg, 0.087 mmol), malodinitrile (57 mg, 0.87 mmol) and KO^{t}Bu (15 mg, 0.13 mmol) in toluene (5 mL) was stirred overnight at room temperature. The solvent was evaporated and the yellow solid residue dissolved in dichloromethane and filtrated. The solvent was then removed and the resulting solid washed with cold hexane to give the pure product as a yellow powder (35 mg, 0.058 mmol, 67 % yield).). Anal. Calcd for $C_{27}H_{27}N_4Au\cdot H_2O$ (622.5): C, 52.09; H, 4.50; N, 9.00. Found: C, 52.43; H, 4.10; N, 9.74. IR (cm^{-1}): ν(C≡N) 2237 (w). ^{1}H NMR (CD_2Cl_2, 300.13 MHz): δ 8.81 (s, 2 H, H^2), 7.85 (d, $^4J_{H\text{-}H}$

= 1.9 Hz, 2 H, H^8), 7.65 (d, $^3J_{H\text{-}H}$ = 8.2 Hz, 2 H, H^5), 7.39 (dd, $^3J_{H\text{-}H}$ = 8.2 Hz, $^4J_{H\text{-}H}$ = 1.9 Hz, 2 H, H^6), 3.68 (s, 1 H, H^{10}), 1.39 (s, 18 H, ^{t}Bu). $^{13}C\{^1H\}$ NMR (CD_2Cl_2, 75.48 MHz): δ 167.3 (s, C^9), 157.4 (s, $C^{3/4}$), 157.1 (s, $C^{3/4}$), 144.9 (s, C^7), 139.2 (s, C^2), 130.9 (s, C^8), 126.6 (s, C^5), 125.4 (s, C^6), 116.1 (s, C^{11}), 36.2 (s, CMe$_3$), 31.3 (s, CMe_3), -3.2 (s, C^{10}).

(C^N^{py}^C)Au{CH(CN)$_2$} (2b)

A mixture of (C^N^{py}^C)AuCl (50 mg, 0.087 mmol), malodinitrile (57 mg, 0.87 mmol) and KO^{t}Bu (15 mg, 0.13 mmol) in toluene (5 mL) was heated overnight at 80^{o}C. The product was isolated as described for **2a**, as a yellow powder (41 mg, 0.068 mmol, 78 % yield).). Anal. Calcd for $C_{27}H_{27}N_3Au$ (603.5): C, 55.72; H, 4.68; N, 6.96. Found: C, 55.32; H, 4.54; N, 7.09. IR (cm^{-1}): ν(C≡N) 2233 (w). ^{1}H NMR (CD_2Cl_2, 300.13 MHz): δ 7.89 (t, $^3J_{H\text{-}H}$ = 8.2 Hz, 1 H, H^1), 7.85 (d, $^4J_{H\text{-}H}$ = 1.9 Hz, 2 H, H^8), 7.55 (d, $^3J_{H\text{-}H}$ = 8.2 Hz, 2 H, H^5), 7.45 (d, $^3J_{H\text{-}H}$ = 8.2 Hz, 2 H, H^2), 7.35 (dd, $^3J_{H\text{-}H}$ = 8.2 Hz, $^4J_{H\text{-}H}$ = 1.9 Hz, 2 H, H^6), 3.64 (s, 1 H, H^{10}), 1.43 (s, 18 H, ^{t}Bu). $^{13}C\{^1H\}$ NMR (CD_2Cl_2, 75.48 MHz): δ 166.4 (s, C^9), 164.6 (s, $C^{3/4}$), 156.1 (s, $C^{3/4}$), 147.2 (s, C^7), 143.6 (s, C^1), 130.3 (s, C^8), 126.1 (s, C^5), 125.1 (s, C^6), 117.2 (s, C^2), 116.6 (s, C^{11}), 36.1 (s, CMe$_3$), 31.5 (s, CMe_3), -3.6 (s, C^{10}).

(C^N^{pz}^C) Au{CH(C(O)Me)$_2$} (3a)

The complex was made following the procedure for **2a**, from (C^N^{pz}^C)AuCl (50 mg, 0.087 mmol), acetylacetone (87 mg, 0.87 mmol) and KO^{t}Bu (12 mg, 0.10 mmol) as a yellow powder (48 mg, 0.075 mmol, 86 % yield). Anal. Calcd for $C_{29}H_{33}N_2O_2Au$ (638.6): C, 54.55; H, 5.21; N, 4.39. Found: C, 54.66; H, 5.30; N, 4.55. IR (cm^{-1}): ν(C=O) 1677 (i). ^{1}H NMR (CD_2Cl_2, 300.13 MHz): δ 8.85 (s, 2 H, H^2), 7.95 (d, $^4J_{H\text{-}H}$ = 1.9 Hz, 2 H, H^8), 7.68 (d, $^3J_{H\text{-}H}$ = 8.2 Hz, 2 H, H^5), 7.36 (dd, $^3J_{H\text{-}H}$ = 8.2 Hz, $^4J_{H\text{-}H}$ = 1.9 Hz, 2 H, H^6), 4.96 (s, 1 H, H^{10}), 2.29 (s, 6 H, H^{12}), 1.40 (s, 18 H, ^{t}Bu). $^{13}C\{^1H\}$ NMR (CD_2Cl_2, 75.48 MHz): δ 205.9 (s, C^{11}), 166.7 (s, C^9), 156.8 (s, $C^{3/4}$), 156.6 (s, $C^{3/4}$), 145.8 (s, C^7), 138.9 (s, C^2), 131.3 (s, C^8), 126.1 (s, C^5), 124.7 (s, C^6), 59.9 (s, C^{10}), 36.4 (s, CMe$_3$), 31.9 (s, C^{12}), 31.4 (s, CMe_3). Crystals of **3a** were grown by slow evaporation of a hexane solution.

(C^N^{py}^C)Au{CH(C(O)Me)$_2$} (3b)

A mixture of (C^N^{py}^C)AuCl (50 mg, 0.087 mmol), acetylacetone (87 mg, 0.87 mmol) and KO^{t}Bu (12 mg, 0.10 mmol) was stirred in toluene (5 mL) overnight. The solution was evaporated. The yellow residue was dissolved in dichloromethane and filtrated through celite.

After evaporation to dryness, the solid residue was washed with light petroleum to give the pure product as a pale-yellow powder (40 mg, 0.075 mmol, 86 % yield). Anal. Calcd for $C_{30}H_{34}NO_2Au$ (637.6): C, 56.52; H, 5.37; N, 2.20. Found: C, 56.38; H, 5.46; N, 2.28. IR (cm^{-1}): ν(C=O) 1677. ^{1}H NMR (CD_2Cl_2, 300.13 MHz): δ 7.97 (d, $^4J_{H-H}$ = 1.8 Hz, 2 H, H^8), 7.83 (t, $^3J_{H-H}$ = 8.0 Hz, 1 H, H^1), 7.56 (d, $^3J_{H-H}$ = 8.1 Hz, 2H, H^5), 7.45 (d, $^3J_{H-H}$ = 8.0 Hz, 2H, H^2), 7.31 (dd, $^3J_{H-H}$ = 8.1 Hz, $^4J_{H-H}$ = 1.8 Hz. 2 H, H^6), 4.69 (s, 1 H, H^{10}), 2.31 (s, 6 H, H^{12}), 1.41 (s, 18 H, ^{t}Bu). ^{13}C{^{1}H} NMR (CD_2Cl_2, 75.48 MHz): δ 205.8 (s, C^{11}), 165.2 (s, C^9), 163.3 (s, $C^{3/4}$), 154.9 (s, $C^{3/4}$), 147.5 (s, C^7), 142.3 (s, C^1), 130.3 (s, C^8), 125.1 (s, C^5), 123.8 (s, C^6), 116.3 (s, C^2), 59.2 (s, C^{10}), 35.7 (s, CMe$_3$), 31.3 (s, C^{12}), 31.0 (s, CMe_3).

(C^N^{pz}^C)Au{CH(CO$_2$Et)$_2$} (4)

Following the procedure given for **2a**, the compound was made from (C^N^{pz}^C)AuCl (50 mg, 0.087 mmol), diethylmalonate (139 mg, 0.87 mmol) and KO^{t}Bu (15 mg, 0.13 mmol) as a yellow powder (37 mg, 0.053 mmol, 61 % yield). Anal. Calcd for $C_{31}H_{37}N_2O_4Au$ (698.6): C, 53.30; H, 5.34; N, 4.01. Found: C, 53.17; H, 5.35; N, 4.03. IR (cm^{-1}): ν(C=O) 1737; 1732 (i). ^{1}H NMR (CD_2Cl_2, 300.13 MHz): δ 8.81 (s, 2 H, H^2), 8.03 (d, $^4J_{H-H}$ = 1.9 Hz, 2 H, H^8), 7.65 (d, $^3J_{H-H}$ = 8.2 Hz, 2 H, H^5), 7.34 (dd, $^3J_{H-H}$ = 8.2 Hz, $^4J_{H-H}$ = 1.9 Hz, 2 H, H^6), 4.96 (s, 1 H, H^{10}), 4.09 (m, 4 H, H^{12}), 1.40 (s, 18 H, ^{t}Bu), 1.13 (t, $^3J_{H-H}$ = 7.5 Hz, 6 H, H^{13}). ^{13}C{^{1}H} NMR (CD_2Cl_2, 75.48 MHz): δ 171.3 (s, C^{11}), 167.8 (s, C^9), 157.0 (s, $C^{3/4}$), 156.6 (s, $C^{3/4}$), 145.3 (s, C^7), 138.7 (s, C^2), 132.3 (s, C^8), 125.9 (s, C^5), 124.5 (s, C^6), 60.9 (s, C^{12}), 38.1 (s, C^{10}), 36.2 (s, CMe$_3$), 31.4 (s, CMe_3), 14.6 (s, C^{13}).

Synthesis of (C^N^{pz}^C)Au{CH$_2$C(O)Ph} (5)

A mixture of (C^N^{pz}^C)AuCl (0.027 g, 0.047 mmol), KO^{t}Bu (0.007 g, 0.056 mmol) and acetophenone (0.056 g, 0.470 mmol) was heated at 80 °C in toluene (3 mL) overnight. The solution was evaporated. The yellow solid residue was dissolved in dichloromethane and filtrated through celite. After evaporation of the dichloromethane and addition of cold hexane (2 mL) a yellow precipitate formed which was collected and dried to give the pure product as a yellow powder (0.029 g, 0.044 mmol, 94 % yield). Anal. Calcd for $C_{32}H_{33}N_2OAu$ (658.6): C, 58.36; H, 5.05; N, 4.25. Found: C, 58.47; H, 5.15; N, 4.30. IR (cm^{-1}): ν(C=O) 1654. ^{1}H NMR (CD_2Cl_2, 300.13 MHz): δ 8.79 (s, 2 H, H^2), 8.11 (dm, $^3J_{H-H}$ = 9.0 Hz, 2 H, H^{13}), 7.93 (d, $^4J_{H-H}$ = 1.9 Hz, 2 H, H^8), 7.64 (d, $^3J_{H-H}$ = 8.2 Hz, 2 H, H^5), 7.38 (tm, $^3J_{H-H}$ = 7.5 Hz, 1 H, H^{15}), 7.27-7.34 (m, 4 H, H^6 + H^{14}), 3.65 (s, 2 H, H^{10}), 1.38 (s, 18 H, ^{t}Bu). ^{13}C{^{1}H} NMR

(CD_2Cl_2, 75.48 MHz): δ 201.4 (s, C^{11}), 166.6 (s, C^{9}), 156.2 (s, $C^{3/4}$), 156.1 (s, $C^{3/4}$), 146.0 (s, C^{7}), 139.3 (s, C^{12}), 138.7 (s, C^{2}), 132.6 (s, C^{15}), 131.3 (s, C^{8}), 129.0 (s, C^{13}), 128.6 (s, C^{14}), 126.0 (s, C^{5}), 124.3 (s, C^{6}), 36.2 (s, CMe$_3$), 31.5 (s, CMe_3), 30.2 (s, C^{10}).

(C^N^{pz}^C)Au{$CH_2C(O)Me$} (6a)

A mixture of (C^N^{pz}^C)AuCl (50 mg, 0.087 mmol) and K_2CO_3 (0.024 g, 0.174 mmol) was stirred in refluxing acetone (5 mL) overnight. The solution was evaporated to dryness, and the yellow residue was dissolved in dichloromethane and filtrated through celite. After evaporation to dryness, the yellow solid was washed with cold hexane to give the pure product as a yellow powder (46 mg, 0.077 mmol, 87 % yield). Anal. Calcd for $C_{27}H_{31}N_2OAu$ (596.2): C, 54.36; H, 5.24; N, 4.70. Found: C, 54.28; H, 5.30; N, 4.75. IR (cm^{-1}): ν(C=O) 1667 (i). ^{1}H NMR (CD_2Cl_2, 300.13 MHz): δ 8.82 (s, 2 H, H^2), 7.97 (d, $^4J_{H-H}$ = 1.9 Hz, 2 H, H^8), 7.66 (d, $^3J_{H-H}$ = 8.2 Hz, 2 H, H^5), 7.33 (dd, $^3J_{H-H}$ = 8.2 Hz, $^4J_{H-H}$ = 1.9 Hz, 2 H, H^6), 3.11 (s, 2 H, H^{10}), 2.23(s, 3 H, H^{12}), 1.40 (s, 18 H, ^{t}Bu). ^{13}C{^{1}H} NMR (CD_2Cl_2, 75.48 MHz): δ 208.8 (s, C^{11}), 167.3 (s, C^{9}), 155.8 (s, $C^{3/4}$), 155.7 (s, $C^{3/4}$), 145.2 (s, C^{7}), 138.2 (s, C^{2}), 131.4 (s, C^{8}), 125.5 (s, C^{5}), 123.7 (s, C^{6}), 35.5 (s, CMe$_3$), 34.9 (s, C^{10}), 30.9 (s, CMe_3), 30.5 (s, C^{12}). Crystals suitable for X-Ray diffraction analysis were grown by slow evaporation of a concentrated solution in acetone.

Synthesis of (C^N^{py}^C) Au{$CH_2C(O)Me$} (6b)

A mixture of (C^N^{py}^C)AuCl (0.050 g, 0.087 mmol) and KO^{t}Bu (0.015 g, 0.13 mmol) in acetone (10 mL) was heated to reflux for 2 d. The volatiles were evaporated under vacuum. The residue was dissolved in dichloromethane (10 mL) and filtrated through celite. Slow diffusion of EtOH (10mL) into the dichloromethane solution gave the product as a pale-yellow microcrystalline solid (0.028 g, 87 % yield). Anal. Calcd for $C_{28}H_{32}NOAu.H_2O$ (613.6): C, 54.81; H, 5.59; N, 2.28. Found: C, 54.81; H, 5.78; N, 2.44. IR (cm^{-1}): ν(C=O) 1674 (i). ^{1}H NMR (CD_2Cl_2, 300.13 MHz): δ 7.96 (s, br, 2 H, H^8), 7.76 (t, $^3J_{H-H}$ = 7.9 Hz, 1 H, H^1), 7.53 (d, $^3J_{H-H}$ = 8.1 Hz, 2H, H^5), 7.40 (d, $^3J_{H-H}$ = 7.9 Hz, 2H, H^2), 7.28 (d, br, 2 H, H^6), 3.02 (s, 2 H, H^{10}), 2.23 (s, 3 H, H^{12}), 1.40 (s, 18 H, ^{t}Bu). ^{13}C{^{1}H} NMR (CD_2Cl_2, 75.48 MHz): δ 209.4 (s, C^{11}), 166.5 (s, C^{9}), 162.9 (s, $C^{3/4}$), 154.4 (s, $C^{3/4}$), 147.6 (s, C^{7}), 141.7 (s, C^{1}), 130.9 (s, C^{8}), 125.0 (s, C^{5}), 123.4 (s, C^{6}), 116.0 (s, C^{2}), 35.4 (s, CMe$_3$), 34.6 (s, C^{10}), 31.0 (s, CMe_3), 30.4 (s, C^{12}).

(C^N^{pz}^C)Au(trifluoroacetate) (7a)

A mixture of (C^N^{pz}^C)AuCl (200 mg, 0.348 mmol) and AgOAc^F (92 mg, 0.417 mmol) was stirred overnight in CH_2Cl_2 (20 mL). The solution was filtrated through celite. Evaporation to dryness afforded a yellow solid that was washed with Et_2O to give the pure product (190 mg, 0.291 mmol, 84 % yield). Anal. Calcd for $C_{26}H_{26}N_2O_2F_3Au$ (652.6): C, 47.86; H, 4.02; N, 4.29. Found: C, 47.75; H, 3.91; N, 4.17. IR (cm^{-1}): ν(C=O) 1727 (m). ^{1}H NMR (CD_2Cl_2, 300.13 MHz): δ 8.70 (s, 2 H, H^2), 7.61 (d, $^3J_{H\text{-}H}$ = 8.2 Hz, 2 H, H^5), 7.43 (d, $^4J_{H\text{-}H}$ = 1.7 Hz, 2 H, H^8), 7.38 (dd, $^3J_{H\text{-}H}$ = 8.2 Hz, $^4J_{H\text{-}H}$ = 1.7 Hz, 2 H, H^6), 1.33 (s, 18 H, ^{t}Bu). ^{13}C{^{1}H} NMR (CD_2Cl_2, 75.48 MHz): δ 170.6 (s, *C*^{9}), 158.2 (s, *C*$^{3/4}$), 157.3 (s, *C*$^{3/4}$), 141.9 (s, *C*^{7}), 138.5 (s, *C*^{2}), 130.0 (s, *C*^{8}), 125.8 (s, *C*^{5}), 125.3 (s, *C*^{6}), 35.5 (s, *C*(CH$_3$)$_3$), 30.7 (s, C(*C*H$_3$)$_3$). ^{19}F{^{1}H} NMR (CD_2Cl_2, 282.38): δ -73.75 (s, C*F*$_3$CO$_2$Au).

(C^N^{pz}^C)AuCH$_3$ (8a)

A mixture of (C^N^{pz}^C)AuOAc^F (50 mg, 0.077 mmol) was dissolved in THF (10 mL). A solution of MeMgBr in 2-MeTHF (0.11 mL, 0.38 mmol) was added dropwise at -78 °C. After completion of the addition the reaction was kept at room temperature for 3 h. THF was evaporated and the residue dissolved in CH_2Cl_2. The dichloromethane phase was washed with water, dried over Na_2SO_4 and filtered. Evaporation to dryness afforded a yellow solid that was washed with hexane to give the pure product (31 mg, 0.056 mmol, 73 % yield). Anal. Calcd for $C_{25}H_{29}N_2Au$ (554.5): C, 54.15; H, 5.27; N, 5.05. Found: C, 54.21; H, 5.18; N, 5.16. ^{1}H NMR (CD_2Cl_2, 300.13 MHz): δ 8.84 (s, 2 H, H^2), 7.74 (d, $^4J_{H\text{-}H}$ = 1.7 Hz, 2 H, H^8), 7.68 (d, $^3J_{H\text{-}H}$ = 8.2 Hz, 2 H, H^5), 7.32 (dd, $^3J_{H\text{-}H}$ = 8.2 Hz, $^4J_{H\text{-}H}$ = 1.7 Hz, 2 H, H^6), 1.39 (s, 21 H, ^{t}Bu + H^{10}). ^{13}C{^{1}H} NMR (CD_2Cl_2, 75.48 MHz): δ 168.1 (s, *C*^{9}), 155.8 (s, *C*$^{3/4}$), 155.5 (s, *C*$^{3/4}$), 146.2 (s, *C*^{7}), 138.6 (s, *C*^{2}), 131.2 (s, *C*^{8}), 126.0 (s, *C*^{5}), 124.0 (s, *C*^{6}), 35.9 (s, *C*Me$_3$), 31.5 (s, C*Me*$_3$), 3.7 (s, *C*^{10}).

(C^N^{py}^C)AuCH$_3$ (8b)

The procedure described for **8a** gave **8b** as a pure yellow solid (37 mg, 0.067 mmol, 87 % yield). ^{1}H NMR (CD_2Cl_2, 300.13 MHz): 7.81 (t, $^3J_{H\text{-}H}$ = 8.2 Hz, 1 H, H^1), 7.75 (d, $^4J_{H\text{-}H}$ = 1.9 Hz, 2 H, H^8), 7.60 (d, $^3J_{H\text{-}H}$ = 8.2 Hz, 2 H, H^5), 7.49 (d, $^3J_{H\text{-}H}$ = 8.2 Hz, 2 H, H^2), 7.28 (dd, $^3J_{H\text{-}H}$ = 8.2 Hz, $^4J_{H\text{-}H}$ = 1.9 Hz, 2 H, H^6), 1.39 (s, 18 H, ^{t}Bu), 1.33 (s, 3 H, H^{10}).

■ ASSOCIATED CONTENT

Supporting Information

For details about X-ray crystallography, photophysical properties, theoretical calculations. See DOI: CCDC 1552153 (**2a**), 1552155 (**3a**), 1521267 (**6a**), 1552154 (**2b**), 1552156 (**7a**) contain the supplementary crystallographic data for this paper. These data can be obtained free of charge from The Cambridge Crystallographic Data Centre via www.ccdc.cam.ac.uk/data_request/cif.

■ AUTHOR INFORMATION

Corresponding Authors

* J. F.-C., tel. +44 1603 592044; e-mail, J.Fernandez-Cestau@uea.ac.uk

*M.B.: tel, +44 1603 592044; e-mail, m.bochmann@uea.ac.uk.

ORCID

Julio Fernandez-Cestau: 0000-0001-7663-6222

Manfred Bochmann: 0000-0001-7736-5428

Notes

The authors declare no competing financial interest.

■ ACKNOWLEDGMENTS

This work was supported by the European Research Council, M. B. is an ERC Advanced Investigator Award holder (grant no. 338944-GOCAT). We would like to thank the '*Centro de Investigación en Síntesis Química*', Universidad de La Rioja, E-26006, Logroño, Spain, and very especially Prof. E. Lalinde, for their kind assistance with the determination of some of the PL properties of the complexes.

References

(1) Reviews: (a) Bronner, C.; Wenger, O. S. *Dalton Trans*. **2011**, *40*, 12409. (b) Roşca, D.-A.; Wright, J. A.; Bochmann, M. *Dalton Transactions* **2015**, *44*, 20785 – 20807. (c) Kumar, K.; Nevado, C. *Angew. Chem. Int. Ed*. **2017**, *56*, 1994 –2015.

(2) Review: (a) Yam, V. W.-W.; Wong, K. M. C. *Chem. Commun*. **2011**, *47*, 11579-11592. (b) Tang, M.-C.; Chan, C. K.-M.; Tsang, D. P.-K.; Wong, Y.-C.; Chan, M. M.-Y.; Wong, K. M.-C.; Yam, V. W.-W. *Chem. Eur. J*. **2014**, *20*, 15233 – 15241.

(3) Review: Wong , K. M.-C.; Chan, M. M.-Y.; Yam, V. W.-W. *Adv. Mater*. **2014**, *26*, 5558-5568.

(4) Yang, B. Z.; Zhou, X.; Liu, T.; Bai, F. Q.; Zhang, H. X. *J. Phys. Chem. A*, **2009**, *113*, 9396-9403.

(5) Review: Fan, C.; Yang, C.-L. *Chem. Soc. Rev*. **2014**, *43*, 6439-6469.

(6) (a) Au, V. K.-M.; Wong, K. M.-C.; Zhu, N.; Yam, V. W.-W. *J. Am. Chem. Soc*. **2009**, *131*, 9076-9085. (b) To, W. P.; Chan, K. T.; Tong, G. S.; Ma, C.; Kwok, W. M.; Guan, X.; Low, K. H.; Che, C.-M. *Angew. Chem. Int. Ed*. **2013**, *52*, 6648-6652. (c) Hung, F F.; To, W. P.; Zhang, J. J.; Ma, C. S.; Wong, W. Y.; Che, C.-M. *Chem. Eur. J*. **2014**, *20*, 8604-8614. (d) So, G.; Tong, M.; Chan, K. T.; Chang, X. Y.; Che, C.-M. *Chem. Sci*. **2015**, *6*, 3026-3037. (e) Lam, E. S.-H.; Lam, W. H.; Yam, V. W.-W. *Inorg. Chem*. **2015**, *54*, 3624-3630. (f) Gonell, S.; Poyatos, M.; Peris, E. *Dalton Trans*. **2016**, *45*, 5549–5556.

(7) For luminescent gold(III) C^N chelate complexes see: (a) Garg, J. A.; Blacque, O.; Fox, T.; Venkatesan, K.; *Inorg. Chem*. **2010**, *49*, 11463-11472. (b) Garg, J. A.; Blacque, O.; Venkatesan, K.; *Inorg. Chem*. **2011**, *50*, 5430-5441. (c) Zehnder, T. N.; Blacque, O.; Venkatesan, K. *Dalton Trans*. **2014**, *43*, 11959-11972. (d) Szentkuti, A.; Bachmann, M.; Garg, J. A.; Blacque, O.; Venkatesan, K. *Chem. Eur. J*. **2014**, *20*, 2585-2596. (e) Szentkuti, A.; Garg, J. A.; Blacque, O.; Venkatesan K. *Inorg. Chem*. **2015**, *54*, 10748-10760. (f) von Arx, T.; Szentkuti, A.; Zehnder, T. N.; Blacque, O.; Venkatesan, K. *J. Mater. Chem. C*, **2017**, *5*, 3765-3769. (g) Crespo, O.; Gimeno, M. C.; Laguna, A.; Montanel-Perez, S.; Villacampa, M. D. *Organometallics* **2012**, *31*, 5520-5526.

(8) (a) To, W. P.; Tong, G. S. M.; Lu, W.; Ma, C.; Liu, J.; Chow, A. L. F.; Che, C. M. *Angew. Chem. Int. Ed*. **2012**, *51*, 2654-2657. (b) Fung, S. K.; Zou, T.; Cao, B.; Lee, P.-Y.; Fung, Y. M. E.; Hu, D.; Lok, C.-N.; Che, C.-M. *Angew. Chem. Int. Ed*. **2017**, *56*, 3892-3896.

(9) To, W. P.; Tong, G. S. M.; Cheung, C. W.; Yang, C.; Zhou, D.; Che, C. M. *Inorg. Chem*. **2017**, *56*, 5046-5059.

(10) Cutillas, N.; Yellol, G. S.; de Haro, C.; Vicente, C.; Rodriguez, V.; Ruiz, *J. Coord. Chem. Rev*. **2013**, *257*, 2784-2797.

(11) Zou, T. T.; Lum, C. T.; Lok, C. N.; Zhang, J. J.; Che, C. M. *Chem. Soc. Rev*. **2015**, *44*, 8786-8801.

(12) (a) Wong , K. M.-C.; Hung , L.-L.; Lam , W. H.; Zhu , N.; Yam, V. W.-W. *J. Am. Chem. Soc*. **2007**, *129*, 4350-4365. (b) Au, V. K. M.; Wong, K. M.-C.; Tsang, D. P. K.; Chan, M. Y.; Zhu, N.; Yam, V. W.-W. *J. Am. Chem. Soc*. **2010**, *132*, 14273-14278. (c) Au, V. K.-M.; Tsang, D. P. K.; Wog, K. M. C.; Chan, M. Y.; Zhu, N.; Yam. V. W.-W. *Inorg. Chem*. **2013**, *52*, 12713-12725. (d) Tang, M. C.; Tsang, D. P. K.; Chan, M. M. Y.; Wong, K. M. C.; Yam, V. W.-W. *Angew. Chem. Int. Ed*. **2013**, *52*, 446-449. (e) Hung. L. L.; Lam, W. H.; Wong, K. M. C.; Cheng, E. C. C.; Zhu, N. Y.; Yam, V. W.-W. *Inorg. Chem. Front*. **2015**, *2*, 453-466. (f) Siu, S. K. L.; Po, C.; Yim, K.-C.; Au, V. K.-M.; Yam, V. W.-W. *Crystal Engin. Commun*. **2015**, *17*, 8153-8162.

(13) Fernandez-Cestau, J.; Bertrand, B.; Blaya, M.; Jones, G. A.; Penfold, T. J.; Bochmann, M. *Chem. Commun*. **2015**, *51*, 16629–16632.

(14) Au(III) halide complexes based on C^C^N pincers also show phosphorescence at room temperature: Kumar, R.; Linden, A.; Nevado, C. *Angew. Chem. Int. Ed*. **2015**, *54*, 14287 –14290.

(15) Bertrand, B.; Fernandez-Cestau, J.; Angulo, J.; Cominetti, M. M. D.; Waller, Z. A. E.; Searcey, M.; O'Connell, M. A.; Bochmann, M. *Inorg. Chem*. **2017**, *56*, 5728−5740.

(16) L. Currie, J. Fernandez-Cestau, L. Rocchigiani, B. Bertrand, S. J. Lancaster, D. L. Hughes, H. Duckworth, S. T. E. Jones, D. Credgington, T. J. Penfold, M. Bochmann, *Chem Eur. J.* **2017**, *23*, 105-113.

(17) While this work was in progress, the photoluminescence of framework-modified pyridine-based (C^N^{py}^C) gold methyl complexes was reported, see ref. 9.

(18) Roşca, D.-A.; Smith D. A.; Bochmann, M. *Chem. Commun*. **2012**, *48*, 7247-7249.

(19) Panunzi, A.; Roviello, G.; Ruffo, F. *Organometallics* **2002**, *21*, 3503-3505.

(20) (a) Komiya, S.; Kochi, J. K.; *J. Am. Chem. Soc*. **1977**, *99*, 3695-3704. (b) Vicente, J.; Bermudez, M. D.; Carrion, F. J.; Jones, P. G. *J. Organomet. Chem*. **1996**, *508*, 53-57.

(21) Venugopal, A.; Ghosh, M. K.; Jürgens, H.; Törnroos, K. W.; Swang, O.; Tilset, M.; Heyn, R. H. *Organometallics* **2010**, *29*, 2248–2253.

(22) Smith, D. A.; Rosca, D.-A.; Bochmann, M. *Organometallics* **2012**, *31*, 5998−6000.

(23) Langseth, E.; Görbitz, C. H.; Heyn, R. H.; Tilset, M. *Organometallics* **2012**, *31*, 6567−6571.

(24) (a) Walker, I. C.; Palmer, M. H.; Hopkirk, A. *Chem. Phys*. **1989**, *141*, 365-378. (b) Walker, I. C.; Palmer, M. H. *Chem. Phys*. **1991**, *153*, 169-187.

(25) Pintus, A.; Rocchigiani, L.; Fernandez-Cestau, J.; Budzelaar, P. H. M.; Bochmann, M. *Angew. Chem. Int. Ed*. **2016**, *55*, 12321-12324.